Organic & Biomolecular Chemistry

Accepted Manuscript

ROYAL SOCIETY OF CHEMISTRY

www.rsc.org/obc

Organic &
Biomolecular Chemistry

EDGE

View Article Online

View journal

Cite this:

DOI: 10.1039/*******

Stability and Bioactivity of Thrombin Binding Aptamers Modified with D-/L-Isothymidine in the Loop Regions

Baobin Cai, Xiantao Yang, Lidan Sun, Xinmeng Fan, Liyu Li, Hongwei Jin, Yun Wu, Zhu Guan, Liangren Zhang, Lihe Zhang, Zhenjun Yang*

Thrombin binding aptamer (**TBA**) is a 15-mer single-strand DNA that was identified by SELEX screening technology. It adopts a chair-type antiparallel G-quadruplex and can specifically interact with thrombin, thus inhibiting blood coagulation. Isonucleoside (**isoNA**) is a type of nucleoside isomer in which the base is shifted to 2'-positions of the glycosyl group, endowed with the ability of modulating local conformation of nucleotides, and **L-isoNA** could alter the conformation more due to the inversion of glycosyl configuration. Incorporation of L-isothymidine (**L-isoT**) at T3, T9, T12 positions and **D-isoT** at T7 position in **TBA**'s loop regions promoted the formation of G-quadruplex, resulted in enhanced affinity with thrombin and increased anticoagulant effect. Computer simulation indicated **TBA-12L** showed the strongest binding with thrombin, which was consistent with experimental results. The bioactivity of double **isoNA** incorporated **TBA** with **D-IsoT** at T7 and **L-IsoT** at T12 was comparable to that of **TBA-12L**, suggesting the T12 of **TBA** was very important in interaction with thrombin. Our study also suggested that **TBA** might interact with two thrombin molecules through the T3T4 and T12T13 loop regions, but the second bonding didn't show additional biological effect.

Received 25th June 2014

Accepted ****** 2014

DOI: 10.1039/**********

www.rsc.org/obc

Department of Medical Chemistry, State Key Laboratory of Natural and Biomimetic Drugs, School of Pharmaceutical Sciences, Peking University, Beijing 100191, PR China. E-mail:yangzj@bjmu.edu.cn

View Article Online
Organic & Biomolecular Chemistry
EDGE Atricle

1. Introduction

Many genes contain G nucleotide rich sequences, which can form the G-quadruplex structure. G-quadruplex is a unique class of highly-ordered nucleic acid structures with many types of folding topologies and molecularities[1-6]. These highly ordered structures have been exploited for the identification of ligands specifically interacting with proteins[7-13]. One well-known example is the thrombin binding aptamer (**TBA**). **TBA** is a 15-mer DNA oligonucleotide with the sequence of 5'-GGT TGG TGT GGT TGG-3', which was discovered in 1992 by Bock.[14] It shows activity of inhibiting fibrin-clot formation by binding to the thrombin protein with high selectivity and affinity. NMR and X-ray structural studies showed that **TBA** forms an intramolecular, chair-like antiparallel G-quadruplex conformation[15]. The G-quadruplex consists of three parts: two G-quadruplexes, the central TGT loop and two TT loops (Figure 1a). However, some differences were observed in the topology revealed by X-ray study from that of NMR study. NMR studies showed the TGT loop spans a wide groove of the quadruplex helix and TT loops span the two narrow grooves[16,17], whereas X-ray studies indicated the TT loops span the wide grooves and the central TGT loop spans the narrow grooves[18]. X-ray studies indicated that inhibition of fibrinogen-clotting is the result of specific blocking of the thrombin anion exosite I by an interaction involving the central TGT loop (Figure 1b). The two TT loops are involved in ionic interactions with the electropositive heparin binding site of a second thrombin molecule in the crystals to compensate the residual negative charge of the aptamer. In contrast, NMR studies indicated that the two TT loops interact with the thrombin anion exosite I (Figure 1c), while the TGT loop is in close proximity to the heparin binding site of a neighboring thrombin molecule. To demonstrate the binding mode between **TBA** and thrombin, extensive studies on the structure of **TBA** and its complex with thrombin had been carried out[15-21]. In addition, X-ray structure study of modified **TBA**s was performed to explain the binding mode of **TBA** and thrombin.[22]

View Article Online
Organic & Biomolecular Chemistry
EDGE Atricle

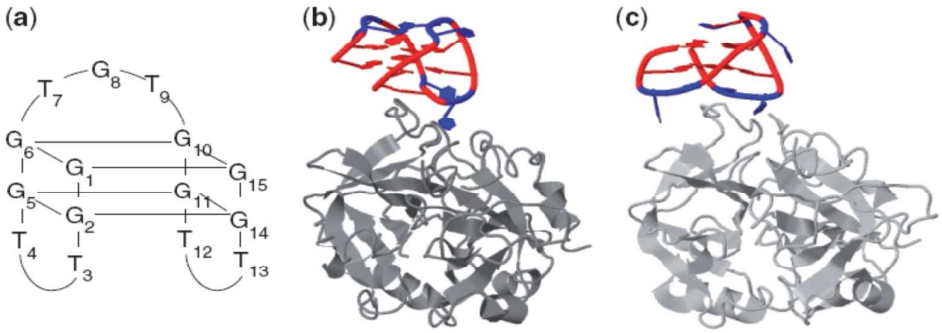

Figure 1. Quadruplex structure of the thrombin binding aptamer (**TBA**) (a), and its interaction with the thrombin anion exosite I according to X-ray (b) and NMR (c) studies. Thrombin is marked in gray, **TBA** is marked in red (**dG**) and blue (**T**).[23]

Since **TBA** is capable of inhibiting the activity of thrombin, many efforts have been made to improve its stability and biological activity. Various chemical modifications have been made, including the modifications with 4-thio-2'-deoxyuridine[24], **LNA** (locked nucleic acid)[25], **UNA** (unlocked nucleic acid)[23], acyclic nucleotide[26], 2'-deoxy-isoguanosine[27], RNA or 2'-*O*-methyl-RNA nucleotides[28], methylphosphonate or phosphorothioate internucleoside linkages[29], partial inversion of **TBA** polarity (5'-3'→3'-5') with an 5'-5' internucleoside linkage[30,31], and changes of loop size and sequence[32]. Most of these modified **TBAs** displayed retained or decreased thermal stability and biological activity compared with unmodified **TBA**. However, a few of the modified **TBAs**, such as 4-thio-2'-deoxyuridine modification at T3, T7, T9 and T13 positions,[24] **UNA** modification at T7 position[23], and [*R*]-acyclic nucleoside (**R-c**) at T12 position[Figure 2],[26a] 2'-deoxy-isoguanosine modification at G11[27] can increase the bioactivity of **TBA**. These results indicated that chemical modifications at the loop regions are more likely to increase the biological activity of **TBA**.

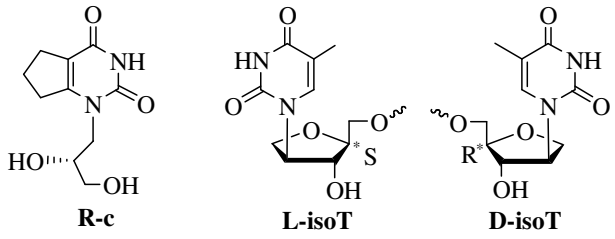

Figure 2. The structure of R-acyclic nucleoside (**R-c**) and D-/L-isothymidine (**D-/L-isoT**)

View Article Online
Organic & Biomolecular Chemistry
EDGE Atricle

Isonucleosides (**isoNAs**) are a type of nucleosides whose bases are shifted from the 1'-position to 2'-position of the glycosyl group (Figure 2). The change of the base position results in the overall conformation change of the nucleoside.[33] In our previous work, we showed that D-/L-**isoNA** modified oligonucleotides could form stable duplex with complementary DNA or RNA oligomers with characteristic tertiary conformation as duplex of DNA/RNA oligomers. A systematic study of the relationship between the conformational alteration around every single nucleotide of antisense oligonucleotide or siRNA and the biological potency has been reported. And the conformational alteration also influences the interactions with proteins, such as nucleases or binding proteins of DNA or RNA oligo. We also found G-rich octaoligo containing another L-form isonucleoside analogue could form a parallel intermolecular G-quadruplex structure.[34]

In this report, we investigated the influence of D-/L-isothymidine (**D-/L-isoT**) modification on the thermal stability, binding affinity and biological activity of **TBA**. Experiments were focused on the loop regions including TGT and both TT loops (Figure 1a), which were verified by X-ray and NMR studies as the main areas that interact with thrombin.[15,19-22] When **L-isoT** was incorporated into **TBA**, the local spatial conformation of **TBA** especially the conformation around the incorporation site was subsequently affected. When the modified nucleotide is part of the target interaction site, the affinity and the biological activity of **TBA**, or the stability of **TBA** in serum could be modulated. Our results indicated that incorporation of **D-/L-isoT** at some positions promoted the formation of G-quadruplex in the loop regions, apparently enhanced the affinity with thrombin, and increased the anticoagulant effect of **TBA**.

2. Experimental Detail

The **TBA** and **D-/L-isoT** modified **TBA**s were synthesized on ABI 394 automated RNA/DNA synthesizer (**IsoT** phosphoramidite monomers and **isoT**-modified oligonucleotides were synthesized by our laboratory according to the literature procedure using standard phosphoramidite chemistry).[34] The purity of all oligonucleotides was verified by Capillary Gel Electrophoresis and polypropylene gel electrophoresis and determined to be

View Article Online
Organic & Biomolecular Chemistry
EDGE Atricle

90% or greater, and the oligonucleotide compositions were confirmed by MALDI–TOF-MS spectrometry.

Melting curve analysis of TBAs

Oligonucleotides were dissolved in a buffer containing 100 mM potassium chloride and 10 mM sodium cacodylate, pH 7.4. Oligonucleotide concentrations were measured by Nanodrop 2000 UV spectrometer. The samples were denatured by heating at 90 ^{o}C for 5 min and then slowly cooled to room temperature. Absorbance versus temperature curves were obtained by the melting method detected at 295 nm[16] in the temperature range of 20-90 ^{o}C on a Beckman DU 800 spectrophotometer equipped with a six-position microcell holder and a thermo programmer. The reversibility of transitions was ensured for all samples by measurement of heating and cooling profiles (data not shown). Three different heating rates (1.0, 0.5 and 0.3 ^{o}C/min) were tested to avoid hysteresis phenomena. The rate of 0.3 ^{o}C/min was selected because under which the melting and annealing curves were reproducible and strictly superimposable. The lack of hysteresis phenomena implied that the dissociation and association process of quadruplex was in a state of thermodynamic equilibrium.[17]

CD measurement

CD spectra of **TBA** and **isoT** modified **TBA**s were obtained with Jasco J610 spectrometer (Japan) using 0.5 ml quartz cuvettes with a 2 mm path length. The concentrations of all oligonucleotides were 7.14 μM. The oligonucleotides were dissolved in the buffer, which contained 138 mM NaCl, 2.7 mM KCl, 10 mM Na_2HPO_4, 1.76 mM KH_2PO_4, pH 7.4. The measurement was done at 25 ^{o}C and the wavelength ranged from 220 nm to 320 nm. Data were smoothed using the system software. To study the secondary structure changes induced by thrombin, **TBA** and **isoT** modified **TBA**s at 4 μM were denatured and then incubated with 20 U thrombin for 30 minutes at 4 ^{o}C. The CD spectra were recorded and presented in Figure 3 (D).

View Article Online
Organic & Biomolecular Chemistry
EDGE Atricle

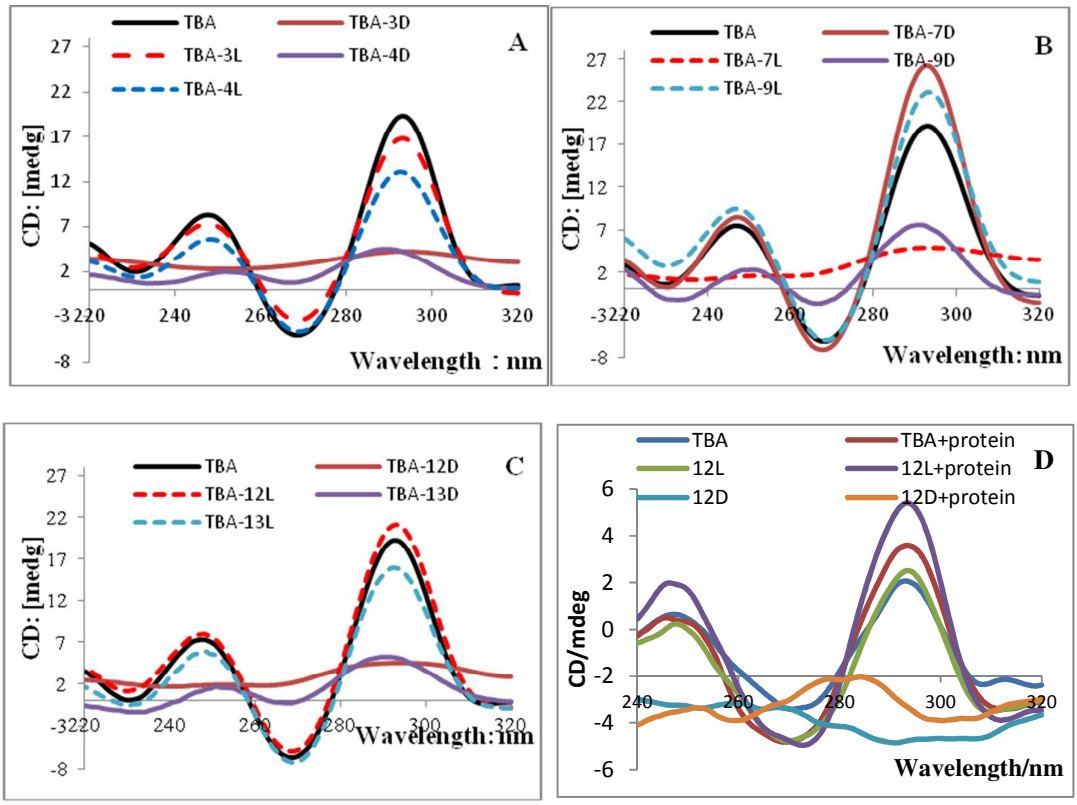

Figure 3. CD spectra of **TBA** (blank solid line) and **D-/L-isoT** modified **TBA**s(A, B and C) 7.14 μM of **TBA** and varients were dissolved in the buffer solution (138 mM NaCl, 2.7 mM KCl, 10 mM Na_2HPO_4,1.76 mM KH_2PO_4, pH 7.4). And the induce effect of the thrombin to **TBA**s(D), the concentration of TBA is 4.0 μM and the thrombin is 20 U.

Serum stability of D-/L-isoT modified TBAs

Nine μl of 20 μM oligonucleotide was placed into the PCR tube followed by the addition of 72 μl of PBS, and the resulting solution was mixed and centrifuged. An aliquot of 9 μl sample was placed in a 200 μl PCR tube as the blank control. 8 μl FBS was added to the remaining 72 μl sample and the sample was placed in an ice-box. After shaking and centrifugation, the total 80 μl sample was divided into eight tubes with 10 μl in each tube. Seven of the eight tubes were placed in a 37 °C water bath, and each tube was removed after incubation for 10, 20, 30, 45, 60, 120 and 180 min. The samples were inactivated at 90 °C for 3 minutes, and placed in a -20 °C refrigerator for storage. Each sample was added with 3 μl 6 × DNA loading buffer and analyzed by electrophoresis.

View Article Online
Organic & Biomolecular Chemistry
EDGE Atricle

Thrombin-aptamer affinity analysis by surface plasmon resonance

Real-time measurement of the interaction between thrombin with **TBA** and **isoT**-modified **TBA**s was performed using a BIAcore 3000 system. Research grade CM5 sensor chips were from GE Healthcare. N-Hydroxysuccinimide, N-ethy-N'-(3-diethylaminopropyl) carbodiimide coupling reagent was used to immobilize thrombin onto the sensor surface using a standard amine-coupling procedure. The running buffer and sample analysis buffer was 10 mM phosphate buffered saline (138 mM NaCl, 2.7 mM KCl, 10 mM Na_2HPO_4, 1.76 mM KH_2PO_4, 0.05% Tween-20), pH 7.4 at 25 ^oC, and all the buffers were filtered and degassed before use. The oligonucleotides were dissolved in the running buffer at different concentrations. **TBA** solutions were sequentially injected over the sensor surface for 3 min at 30 μl/min and 5 min dissociation time. The unbound TBA was removed by treatment with 10 mM aqueous NaOH and the chip was primed before use. For each oligonucleotide, six concentrations were injected by serially diluting samples from 0.05 to 20 μM along with a blank sample containing only running buffer. After each run, the surface was regenerated with 10 mM aqueous NaOH for 20 s at 30 μl/min. The raw data were analyzed to determine the binding constant for each oligonucleotide. To correct for refractive index changes and instrument noise, the responses from the control surface were subtracted from the responses obtained from the reaction surface using biospecific interaction analysis evaluation 4.1. The dissociation constants (K_D) were calculated by global fitting of the six concentrations of **TBA**s over the equation $Y = B\text{max } X/(K\text{d} + X)$, using OriginPro 8.0 software.

The inhibitory effects of isoT modified TBA on thrombin time

The inhibitory effect of **TBA** and the **isoT** modified **TBA**s on the thrombin time was measured with PUN-2048B dual-channel coagulation analyzer (Beijing Poulenc Medical Science and Technology Co., Ltd. China). Venous blood was collected into a tube containing 109 mmol/L sodium citrate as the anticoagulant. The blood was centrifuged for 15 minutes at 3500 rpm to obtain the plasma. The thrombin reagent was pre-incubated with **TBA** or the modified **TBA** at 0.33 μM concentration for 5 min before added to the plasma for the

View Article Online
Organic & Biomolecular Chemistry
EDGE Atricle

measurement of thrombin clotting time. The anti-thrombin effect is assessed by the extra time required for clotting in the presence of aptamers compared with the blank sample.

Computer dynamics simulation

The interactions of **D-/L-isoT** modified **TBA** with thrombin was simulated according the literature[35]. All simulations were performed using the AMBER 11 package utilizing the all-atom force field AMBER99SB. The force field parameters for the isonucleosides **D-isoT** and **L-isoT** were obtained by quantum chemical methods using the Gaussian 09 program. At the B3LYP/ 6-31G* level of theory, we separately optimized the full geometries, and calculated the HF/6-31G* electrostatic potential. The RESP strategy was used to obtain the partial atomic charges. The nonstandard residue in modified **TBA**s was created using the Xleap module. The initial complex structure of **TBA**-thrombin was generated by using the coordinates of the X-ray structure of thrombin and **TBA** (Protein Data Bank code: 4DIH).

The models were explicitly solvated in a rectangular box which extended 10 Å away from any solute atom; 11 Na^+ ions were added to provide electro neutrality. The three systems contained about 11848 (native **TBA**), 11859 (**TBA-12L**), 11867(**TBA-12D**) TIP3P water molecules, respectively. Initially an energy minimization of 1000 steps using the steepest descent algorithm was followed by a 200 ps position-constrained MD simulation in order to equilibrate water and ions. The subsequent free MD simulations were performed for the **TBAs**. All simulations were carried out with periodic boundary conditions for 6 ns at constant temperature (300 K) and pressure (1 atm) and an integration time step of 2 fs was used. Free-energy analysis was performed using the MM_PBSA.py module in AMBER 11 package.

Another crystal structure of **TBA**/thrombin (PDB Code 1HAP) was also used to simulate the interaction between the TGT loops of **TBA** with thrombin[18]. MD simulations were performed with AMBER 11 molecular simulation package[36]. The AMBER99 force field was used to describe the three complexes. To obtain molecular mechanical parameters for the **D/L-isoT**, ab initio quantum chemical methods were employed using the Gaussian 09 program[37]. The geometry was fully optimized and then the electrostatic potentials around

View Article Online
Organic & Biomolecular Chemistry
EDGE Atricle

them were determined at the HF/6-31G* level of theory. The RESP strategy[38] was used to obtain the partial atomic charges. The other modifications, **TBA-7D/**thrombin, **TBA-7L/**thrombin were built on the basis of **TBA/**thrombin using Disovery Studio 2.5 package[39]. Three starting models were solvated in TIP3P water using a octahedral box, of which extended 8 Å away from any solute atom. To neutralize the negative charges of simulated molecules, K^+ counterion was placed next to each phosphate group.

Free-energy analysis was performed using the MM_GBSA scripts supplied by AMBER 11[40-41]. Snapshots from the MD trajectories of the studied system with water and counterions removed were considered for the binding free energy calculations. A total of 100 snapshots were selected at 20 ps intervals from each of the 2.0 ns trajectories.

The root-mean-square deviations (RMSDs) with respect to the starting X-ray structures were calculated to confirm the stability of the trajectory. Three plots of the RMSD values as a function of the simulation time are shown in **Figure 2**. For **TBA-7D/**thrombin the RMSD values gradually increased within about 1.0 ns of simulation, and then remained stable for the rest of the simulation (average RMSD around 2.5 Å). The RMSD of **TBA/**thrombin trajectory showed slow increase during the first 4.0 ns, and achieved equilibrium in the final stage of the simulation.

3. Results and Discussion

The anticoagulant activity in vitro experiments proved that the biological activity of **TBA** modified by **D/L-isoT** improved obviously compared to **TBA**. In order to further reveal the mechanism of enhanced bioactivity of modified **TBA**, and to provide more guidance for future chemical modification of **TBA**, the thermodynamic stability, two-dimensional structure, serum stability, affinity to thrombin and computer dynamics simulation of **D/L-isoT** modified **TBA** with thrombin were performed.

3.1 Anticoagulant effect of the D-/L-isoT modified TBAs

View Article Online
Organic & Biomolecular Chemistry
EDGE Atricle

To investigate the inhibition activities of **isoT**-modified **TBA**s, all modified **TBA**s were tested in a thrombin time assay. As shown in Table 1, **TBA-3L**, **TBA-7D**, **TBA-9L** and **TBA-12L** showed great improvement in the inhibiting activity of thrombin, and their clotting times were 40.5, 37.9, 38.9, and 45.8 s, respectively, compared with that of **TBA** (34.4s). Other modified **TBA**s showed decreased activity of inhibiting thrombin.

Table 1. The dissociation constant (K_D) and anti-anticoagulant effect of **D-/L-isoT** modified **TBAs**.

Name	K_D(μM)	Clotting-time(s)	Anticoagulant effect (s)
blank		19.5	N.A
TBA-U7*		32.6	13.6
TBA	0.96 ± 0.54	34.4	14.9
TBA-3D	4.03 ± 1.56	28.2	8.7
TBA-3L	0.59 ± 0.31	40.5	21.0
TBA-4D	10.41 ± 2.41	27.4	7.9
TBA-4L	6.46 ± 5.73	26.6	7.1
TBA-7D	0.46 ± 0.11	37.9	18.4
TBA-7L	1.69 ± 0.47	31.3	11.8
TBA-9D	1.27 ± 0.28	31.9	12.4
TBA-9L	0.51 ± 0.12	38.9	19.4
TBA-12D	4.69 ± 1.53	27.4	7.9
TBA-12L	0.33 ± 0.11	45.8	26.3
TBA-13D	6.64 ± 2.30	27.5	8.0
TBA-13L	11.86 ± 5.06	26.8	7.3

* The results were reported in literature[23] for **UNA** modified **TBA**, the clotting-time for natural **TBA** and blank are respectively 28.8 s and 19.0 s. The clotting-time for **TBA-U7** prolonged 3.8 s, however the **TBA-12L** prolonged 11.4s compared to natural TBA

3.2 Thermal stability of TBA and IsoT modified TBAs

D-/L-isoT monomers were incorporated as single substitutions at the loop regions of **TBA** at positions 3, 4, 7, 9, 12 and 13. The Tm and ΔTm values are listed in Table 2. The elevated Tm values of modified **TBA** indicated that **D-/L-isoT** modification at relative position can promote the formation of G-quadruplex. As shown in Table 2, **TBA-3L**, **TBA-7D**, **TBA-9L**, **TBA-12L** exhibited elevated *Tm* by 2.5, 5.4, 5.1, 3.1 ^{o}C, respectively, indicating these **D-/L-isoT** modifications promoted the formation of G-quadruplex. As the

View Article Online
Organic & Biomolecular Chemistry
EDGE Atricle

chair-type antiparallel G-quadruplex is essential for the anticoagulant activity of **TBA**, it was likely that these modified **TBA**s may be more active than the parent **TBA**. To improve the stability further, we randomly combined the positions that can improve the thermodynamic stability. It was found that **TBA-3L7D, TBA-3L12L** and **TBA-7D12L** elevated *Tm* by 5.3, 2.9, 6.2 ^{o}C respectively, indicating that double modification could enhance the stability of modified **TBAs**.

Table 2. Sequences and Tm value of **TBA**s with **D-/L-isoT** modification

Name	Sequence	MOLDI TOF		Tm	ΔTm
		Cald.	Found	(^{o}C)	(^{o}C)
TBA	5'-GGTTGGTGTGGTTGG-3'	4726	4728	49.8	
TBA-3D	5'-GG***T$_D$***TGGTGTGGTTGG-3'	4726	4728	51.3	1.5
TBA-3L	5'-GG***T$_L$***TGGTGTGGTTGG-3'	4726	4728	52.3	2.5
TBA-4D	5'-GGT***T$_D$***GGTGTGGTTGG-3'	4726	4728	35.9	-13.9
TBA-4L	5'-GG***T$_L$***TGGTGTGGTTGG-3'	4726	4728	44.5	-5.3
TBA-7D	5'-GGTTGG***T$_D$***GTGGTTGG-3'	4726	4728	55.2	5.4
TBA-7L	5'-GGTTGG***T$_L$***GTGGTTGG-3'	4726	4728	37.1	-12.7
TBA-9D	5'-GGTTGGTG***T$_D$***GGTTGG-3'	4726	4728	38.6	-11.2
TBA-9L	5'-GGTTGGTG***T$_L$***GGTTGG-3'	4726	4728	54.9	5.1
TBA-12D	5'-GGTTGGTGTGG***T$_D$***TGG-3'	4726	4728	50.7	0.9
TBA-12L	5'-GGTTGGTGTGG***T$_L$***TGG-3'	4726	4728	52.9	3.1
TBA-13D	5'-GGTTGGTGTGGT***T$_D$***GG-3'	4726	4728	32.3	-17.5
TBA-13L	5'-GGTTGGTGTGGT***T$_L$***GG-3'	4726	4728	46.5	-3.3
TBA-3L7D	5'-GG***T$_L$***TGG***T$_D$***GTGGTTGG-3'	4726	4728	55.1	5.3
TBA-3L9L	5'-GG***T$_L$***TGGTG***T$_L$***GGTTGG-3'	4726	4728	38.8	-11.0
TBA-3L12L	5'-GG***T$_L$***TGGTGTGG***T$_L$***TGG-3'	4726	4728	52.7	2.9
TBA-7D9L	5'-GGTTGG***T$_D$***G***T$_L$***GGTTGG-3'	4726	4728	35.0	-14.8
TBA-7D12L	5'-GGTTGG***T$_D$***GTGG***T$_L$***TGG-3'	4726	4728	56.0	6.2
TBA-9L12L	5'-GGTTGGTG***T$_L$***GG***T$_L$***TGG-3'	4726	4728	38.7	-11.1
Buffer: 100 mM KCl, 10 mM sodium cacodylate, pH 7.0					

3.3 Analysis of CD spectra

The CD spectra of **TBA** and **D-/L-isoT** modified **TBAs** were obtained to investigate the impact of **isoT** modification on the overall structure of **TBA** (Figure 3). The results were consistent with the Tm value changes. **TBA-3L**, **TBA-7D**, **TBA-9L** and **TBA-12L**, which showed elevated Tm, the intensity of the CD bands increased. While other single-site modified **TBA**s, which showed lowered Tm, resulted in decreased intensity of the CD bands.

In some cases, the bands even disappeared completely compared with the spectrum of the parent **TBA**. A typical chair-type antiparallel G-quadruplex showed two maximal absorption bands at ~250 and 294 nm, and one negative absorption peak at ~270 nm. The configurations of **TBA-3L**, **TBA-7D**, **TBA-9L** and **TBA-12L** were likely similar, because they showed almost the same CD spectral features. The characteristic peaks of **TBA-3D**, **TBA-4D**, **TBA-4L**, **TBA-7L**, **TBA-9D**, **TBA-12D**, **TBA-13D** and **TBA-13L** decreased or even disappeared completely, suggesting that this modification was not suitable to form the chair-type antiparallel G-quadruplex configuration which is essential for the activity of **TBA**. Figure 3D showed the inducing effect of thrombin on the G-quadruplex structure. The difference between **TBA** and **TBA-12L** was small without thrombin, but the signals were stronger and the difference was expanded in the presence of thrombin. It indicated that thrombin could induce **TBA** and **TBA-12L** to form a chair-type anti-parallel G-quadruplex structure, and the effect is more pronounced for **TBA-12L**.

3.4 Serum stability of TBA and D-/L-isoT modified TBAs

We found that most of the unmodified **TBA** was degraded in 1 h in 10% fetal bovine serum, and no **TBA** was detected after 2 hours by electrophoresis. The stability of **TBA-7L** was similar to that of unmodified **TBA**. However, **TBA-7D** was more stable than unmodified **TBA** and **TBA-7L** in 10% fetal bovine serum, as shown by electrophoresis that it can be clearly detected after 2 hours and even after 3 hours. The stability of **TBA-9D**, **TBA-9L** was assayed similarly and **TBA-9L** showed higher stability than **TBA** and **TBA-9D** showed less stability than **TBA** (Figure 4).

View Article Online
Organic & Biomolecular Chemistry
EDGE Atricle

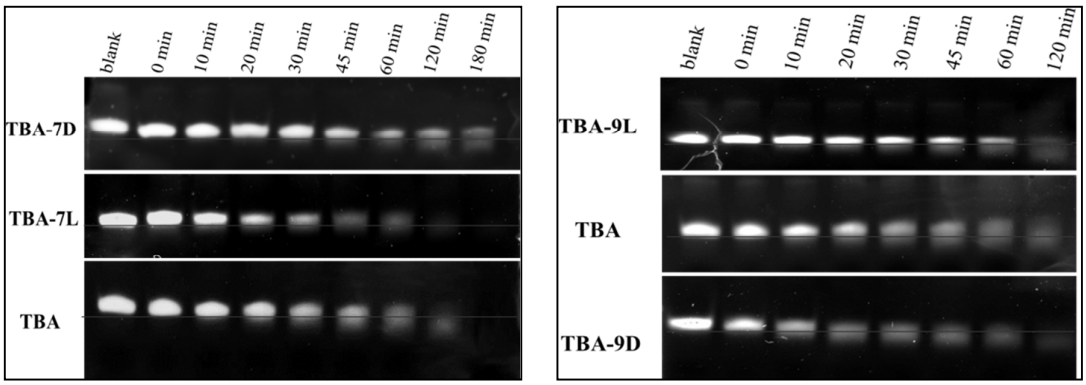

Figure 4. The serum stability of **TBA** and **isoT** modified **TBAs** in 10% FBS.

3.5 Affinity of D-/L-isoT modified TBAs to thrombin

We used surface plasmon resonance (SPR) to study the binding between thrombin and **isoT**-modified **TBA**s. The concentrations of **TBA**s ranged from 0.05 to 20 μM to determine the dissociation constant (K_D). Table 1 shows the dissociation constant (K_D) values of unmodified **TBA** and **isoT** modified **TBAs**, which ranged from 11.86 μM to 0.33 μM. **TBA-3L** (K_D = 0.59 μM), **TBA-7D** (K_D = 0.46 μM), **TBA-9L** (K_D = 0.51 μM) and **TBA-12L** (K_D = 0.33 μM) showed significant improvement of affinity compared with unmodified **TBA**. The affinity of **TBA-12L** (K_D = 0.33 μM) was improved by almost three times compared with that of **TBA** (K_D = 0.96 μM). Both CD and melting curve analysis indicated that **D-/L-isoT** incorporation at certain positions can promote the formation of G-quadruplex, and these modified **TBAs** with more thermodynamically stable G-quadruplex showed higher affinity to thrombin, as exampled by **TBA-12L**. Those modified **TBA**s that formed unstable G-quadruplex structure showed weaker binding to thrombin, which clearly demonstrated the essential role of G-quadruplex in the interactions with thrombin.

3.6 Computer dynamics simulation of the interactions of TBA, TBA-12L, TBA-12D with thrombin

The stability of the **TBA**/thrombin complex was verified by a 4 ns free MD simulation. Another two stable trajectories of modified **TBA**/thrombin complexes (**TBA-12L** and **TBA-12D**) were also produced with the simulation time of 6 ns. The root mean-square deviation (RMSD) plots, with the initial x-ray structure as a reference, were calculated for the

View Article Online
Organic & Biomolecular Chemistry
EDGE Atricle

whole structure in the **TBA** and modified **TBA** quadruplexes (Figure 5). For **TBA** and **TBA-12L**, the RMSD for the whole structure gradually increased during the first 1ns of simulations and then fluctuated around 2.5Å. It was observed that the RMSD of **TBA-12D** kept increasing until 4 ns and fluctuated around 3Å. Compared with the unmodified **TBA** structure, some structure variations have occurred. After the trajectory of **TBA-12D** reached equilibrium, the RMSD of the quadruplex increased to 1.2 Å, which indicated that the **D-isoT** at position 12 decreased the stability of the **TBA** G-quadruplex structure.

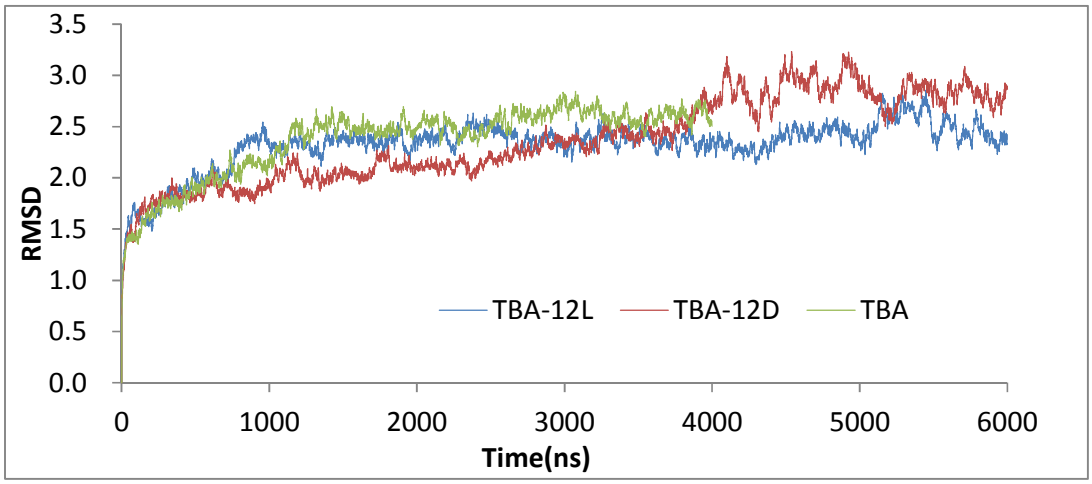

Figure 5. Simulation of the equilibrium structures of **TBA**, **TBA-12D** and **TBA-12L**.

The average structures over the last 2 ns of MD simulations are shown in **Figure 6**. The G-quadruplex of **TBA-12L** is in good agreement with the unmodified **TBA** structure while the G14 and G15 in **TBA-12D** deviated strongly from their equilibrium positions. Obviously, the **TBA-12L** formed similar loop conformations like that of the unmodified **TBA**, leading to more contacts with thrombin. In contrast, the **TBA-12D** exhibited changed loop conformation, which disrupted the binding.

View Article Online
Organic & Biomolecular Chemistry
EDGE Atricle

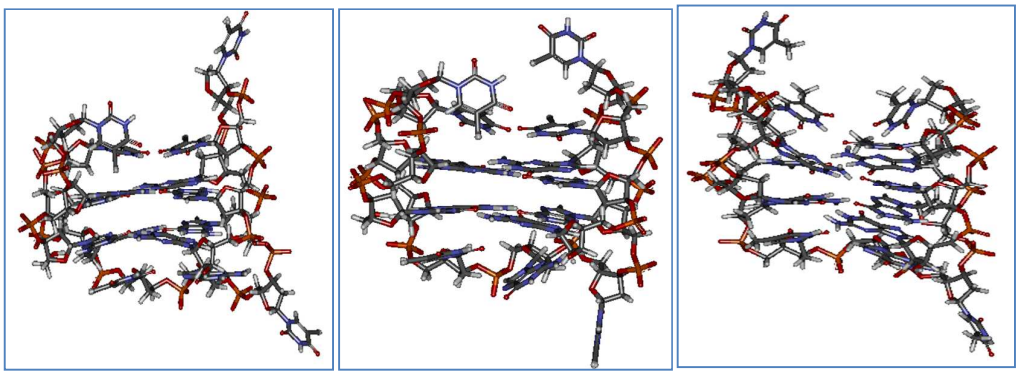

Figure 6. The average structures of **TBA-12L** (left), **TBA** (middle) and **TBA-12D** (right) induced by thrombin.

Interactions between TBA and thrombin

Figure 7 and **Table 3** show the interactions between **TBA** and the exosites I of thrombin. Several protein residues, such as Arg-75, Tyr-76, Arg-77A, Glu-78 and Tyr-117, are involved in the binding of aptamers. Compared with the composite structures of **TBA** and thrombin revealed by X-ray studies, all contacts of **TBA** are conserved during the MD simulations. These interactions have been described clearly in a previous report. [21]

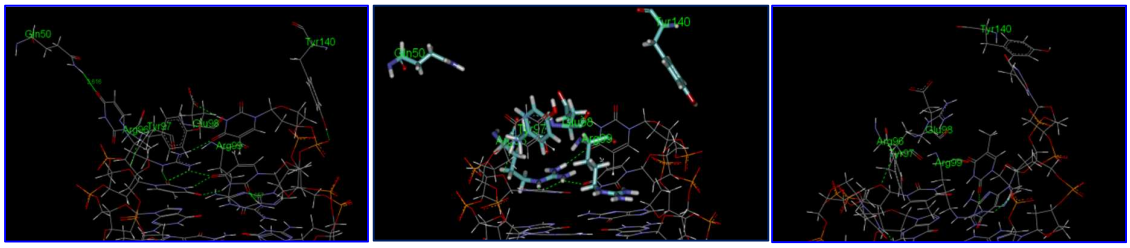

Figure 7. Computer simulation of the interactions of **TBA-12L** (left), **TBA** (middle) or **TBA-12D** (right) with thrombin.

Apart from the interactions revealed in the X-ray structure, additional interactions between **TBA-12L** and the exosite I of thrombin were also formed. In particular, the modification by **L-isoT** changed the orientation of the base and increased the contact surface with thrombin, leading to different interactions with thrombin. The distance between O2 of **L-isoT** and NH_2 group of Glu-27 was 2.6 Å with a hydrogen bond formed. It was also noted that the sugar ring occupied the position of the base and formed hydrophobic interactions with

View Article Online
Organic & Biomolecular Chemistry
EDGE Atricle

Tyr-76. Residue Tyr-117 can form hydrophobic interaction with T4 in the **TBA**-thrombin complex. Interestingly, residue Tyr-117 formed hydrophobic interaction and strong hydrogen bonding with the phosphate oxygen atom of T4 in **TBA-12L**. During the simulation of the interactions of **TBA** and **TBA-12L** with thrombin, the side chain of Arg-77A formed hydrogen bonding with O2 of T13. But the hydrogen bond formed with **TBA-12L** was stronger with a smaller distance of 1.6Å, while the distance was 2.6Å with the unmodified **TBA**.

In contrast, modification with **D-IsoT** at position 12 (**TBA-12D**) disrupted the conformation of modified **TBA** and many contacts were lost during the simulation. Our simulation study indicated **L-isoT** at position 12 increased the binding to the exosite I while **D-isoT** completely destroyed the interactions.

Table 3. Interactions between **TBA** and modified **TBAs** with the exosite I of thrombin

	TBA-nature		**TBA-12L**		**TBA-12D**	
	Aptamer residue	Protin residue	Aptamer residue	Protin residue	Aptamer residue	Protin residue
H-bond	Thy3	Glu77	Thy3	Glu77	-	-
H-bond	Thy4	Arg75	Thy4	Arg75	Thy4	Arg75
H-bond	Thy4	Arg77A	Thy4	Arg77A	-	-
H-bond	Thy13	Arg75	Thy13	Arg75	-	-
H-bond	Thy13	Tyr76	Thy13	Tyr76	Thy13	Tyr76
H-bond	-	-	Thy4	Tyr117	-	-
H-bond	-	-	Iso-12L	Gln29	Iso-12D	Gln29
hydrophobic	Thy3	Ile24, Ile79, Tyr117	Thy3	Ile24, Ile79, Tyr117	-	-
hydrophobic	Thy4	Ile79	Thy4	Ile79	-	-
hydrophobic	Thy12	Tyr76	Iso-12L	Tyr76	-	-
hydrophobic	Thy13	Tyr76	Thy13	Tyr76	-	-

Effects of combined bis-D-/L-isoT modification of TBA on structure and thrombin bonding

As single modification at position T3, T9, T12 with **L-isoT** or position 7 with **D-isoT** promoted the formation of G-quadruplex, we further investigated combined bis-**D-/L-isoT** modification on **TBA** (Table 2). Comparing the average structures (Figure 8), it was found

View Article Online
Organic & Biomolecular Chemistry
EDGE Atricle

that **TBA-3L12L** can form a regular G4 structure. The panel formed by the four guanosines of **TBA-3L12L** is almost same as **TBA.** In contrast, the structure of **TBA-7D9L** was disturbed, and it cannot form a regular G4 structure. However, due to limitations of the MD simulation, this method can't be used to simulate **TBA** variants modified with **bis-D-/L-isoT** in TT and TGT loops.

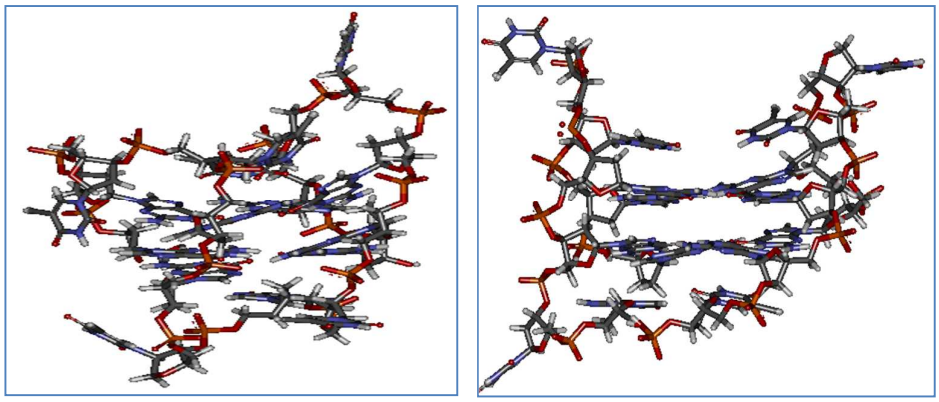

Figure 8. The average structures of **TBA-7D9L** (left) and **TBA-3L12L** (right).

The CD spectrals of combined **bis-D-/L-isoT** modified **TBA** variants are also in consists with the simulation results. As shown by the CD spectra in Figure 9, **TBA-7D12L** and **TBA-3L7D** greatly improved the formation of antiparallel G-quardruplex, compared with **TBA**. And **TBA-7D9L** showed comparable formation of G-quardruplex, but all others almost destroyed G-quardruplex completely.

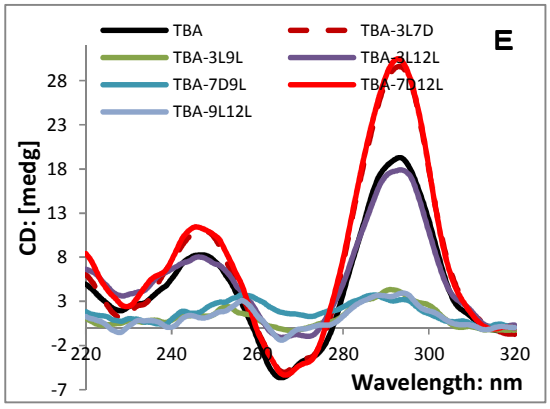

Figure 9. CD spectra of **TBA** (blank solid line) and combined bis-**D-/L-isoT** modified aptamers. The buffer is same as that in Figure 3.

View Article Online
Organic & Biomolecular Chemistry
EDGE Atricle

Some bis-**D-/L-isoT** modified **TBA**, such as **TBA-3L7D** and **TBA-7D12L**, showed significantly improved bioactivity compared with **TBA**. Although they also showed stronger bonding to thrombin, but didn't show increased anticoagulant effect further compared with **TBA-12L** (Table 4).

Table 4. The dissociation constant (K_D) and anti-anticoagulant effect of **TBA** and double **D-/L-isoT** modified **TBA**

Name	K_D (μM)	Clotting-time (s)	Anticoagulant effect (s)
Blank		19.4	
TBA	0.68 ± 0.16	34.3	14.9
TBA-12L	0.31 ± 0.09	45.6	26.2
TBA-3L7D	0.17 ± 0.06	39.3	19.9
TBA-3L9L	0.65 ± 0.15	32.7	13.3
TBA-3L12L	7.81 ± 0.98	27.3	7.81
TBA-7D9L	7.81 ± 0.96	27.3	7.81
TBA-7D12L	0.28 ± 0.09	45.3	25.9
TBA-9L12L	0.84 ± 0.19	33.0	13.6

DISCUSSION

TBAs interact with thrombin specifically and inhibit blood clotting, which are promising drug candidates. Various modifications of **TBA** have been made to increase their stability and bioactivity. In this study, we introduced **D-** or **L-isoT** at different positions of **TBA**, and melting curve analysis revealed that when either **D-** or **L-isoT** was introduced at the positions of T4 and T13, the thermal stability of modified **TBAs** significantly reduced. T4 is close to G5 and T13 is close to G14, and the base of T4 and T13 stacks tightly on the top of G-quadruplex that is composed of G2, G5, G11 and G14. In addition, the hydrogen bonds between T3 and T14 stabilize the G-quadruplex structure[42]. Therefore, when T4 or T13 was substituted by **D-/L-isoT**, the π-π stacking as well as the hydrogen bonds between T4 and T13 were disrupted. As a result, the G-quadruplex structure was destabilized.

Both **D-** and **L-isoT** substitutions at T4 and T13 showed the same decreasing effect on the thermal stability of the modified **TBA**. However, modifications at other locations, such as T3, T7, T9 and T12, showed configuration-dependent effects on thermal stability. When **D-isoT** substitution increased G-quadruplex stability, **L-isoT** would decrease stability, and vice versa. Melting curve analysis indicated **TBA-3L**, **TBA-7D**, **TBA-9L** and **TBA-12L**

View Article Online
Organic & Biomolecular Chemistry
EDGE Atricle

increased stability, while other **D-/L-isoT** modified **TBA**s such as **TBA-3D**, **TBA-9D**, **TBA-7L** and **TBA-12D** decreased stability. These modified **TBAs** with increased stability such as **TBA-3L**, **TBA-7D**, **TBA-9L** and **TBA-12L** also showed stronger CD signals in the featured region (295 nm). The CD signals of these **TBA**s with lower stability decreased or disappeared. The thermodynamically more stable aptamer also showed higher serum stability, indicating the stable G-quadruplex is resistant to nuclease degradation.

The binding kinetic study of the **D-/L-isoT** modified **TBA** aptamers revealed that about half of the **isoT** modifications were tolerated in the loop regions of **TBA** without largely (> 2 fold) affecting the binding affinity (**TBA-3D**, **TBA-3L**, **TBA-7D**, **TBA-7L**, **TBA-9D**, **TBA-9L**, **TBA-12D**, **TBA-12L**). In contrast, the modifications with **D/L-isoT** at T4 and T13 positions abolished or strongly inhibited the interaction with thrombin. It was reported that the **TBA** structure is retained after binding with thrombin. [18, 20] Therefore, the changes in binding constants are likely related with the structural changes as well as the thermal stability of the G-quadruplexes. It was demonstrated that the loop regions of **TBA** are interacting with thrombin[16]. And the biological activity was improved when UNA (Figure 2) was introduced to the T7 of the loop region[25], . Therefore, the loop regions were selected to be modified. From Table 1, the affinity of **TBA-7D** to thrombin was 2 fold higher than that of **TBA**. According to X-ray structure of **TBA** bound to thrombin, T7 is buried in a hydrophobic cluster in the fibrinogen recognition site (Figure 1b)[22, 31]. The increased affinity may thus be attributed to the shift of base from 1' position to 2' position of the glycosyl group, which is favorable for the change of orientation of **isoT-7D** for better quadruplex-protein complex formation. Moreover, **TBA-12L** exhibited the lowest K_D of all studied **TBAs**, and its affinity to thrombin was 3-fold higher than that of unmodified **TBA**. These results suggested that the TT loop also has strong interactions with the active sites of thrombin, and it may be even stronger than the interaction with the central TGT loop. This conclusion is supported by the NMR study. According to the NMR structure, the central loop is not directly involved in the specific interactions with thrombin, and the inhibitory effect is rather the consequence of blocking thrombin anion exosite I by the two TT loops.

View Article Online
Organic & Biomolecular Chemistry
EDGE Atricle

Thrombin clotting time assay showed that the studied **TBAs** possessed various activities (Table 1). A clear correlation between the thermodynamic stability of the G-quadruplex and clotting time can be found. For example, **TBA-3L**, **TBA-7D**, **TBA-9L**, and **TBA-12L** had stable quadruplexes, higher thrombin binding and extended anticoagulant time. Similarly, the thermodynamically unstable **TBA-4D**, **TBA-4L**, **TBA-7L**, **TBA-9D**, **TBA-13D TBA-13L** possessed weaker binding affinity towards thrombin and were biologically inactive. However, the thermal stability of **TBA-3D** (*Tm* = 51.3) and **TBA-12D** (*Tm* = 50.7) were similar or a little higher than **TBA** (*Tm* = 49.8), but their binding affinity towards thrombin and clotting activity were reduced. Therefore, there are other factors affecting the activity of **TBAs**. The UNA modification study indicated that improving the stability of **TBA** did not improve the activity[25]. Our results demonstrated improved stability of the modified **TBA**s mostly led to increased activity. In all cases, decreased stability of modified **TBA**s resulted in reduced biological activity. This observation indicated the stability of the **TBA** is a necessary condition for its biological activity. Because the regions of **TBA** interacting with thrombin are the central TGT and two TT loops[17], the conformation of the nucleotides in these regions was modified to improve the activity. We found replacement with **D-isoT** and **L-isoT** had the opposite effects, i.e., when one increased the activity, the other decreased the activity, and vice versa. These results demonstrated the importance of base orientation in the interaction with the amino acid residues of thrombin.[31, 43]

The interactions of **TBA**, **TBA-12L** and **TBA-12D** with thrombin were also studied by computer simulation, and the results were consistent with our experimental data. The MD simulations clearly depicted the stability of the modified **TBA** structures and their interactions with thrombin were affected by the substitutions of **D-isoT** or **L-isoT** at T12 position of **TBA**. The comparison between the molecular models obtained for the complex with **TBA-12L** and the complex with **TBA-12D** indicated that the base location and orientation were critical for the binding. Furthermore, the resulting models showed that the modified **TBA-12L** made more contacts with thrombin than **TBA-12D** and the detailed interactions (**Table 3**) can well explain the difference of the biological activity. In our models, **L-isoT** led to an extended conformation and extra strong interactions with thrombin were formed. **TBA-12L** formed a

View Article Online
Organic & Biomolecular Chemistry
EDGE Atricle

strong hydrogen bond with Glu-27 and the sugar ring formed hydrophobic interaction with Tyr-76. In addition, residue Tyr-117 formed an extra strong hydrogen bond with the phosphate oxygen atom of T4. These interactions were unique for **TBA-12L** and they can explain the increased biological activity of **TBA-12L**. Moreover, the modification also strengthened the hydrogen bond formed by Arg-77A and T13. For **TBA-12D**, whose conformation is opposite to that of **L-isoT** changed the loop conformation and disrupted the G-quadruplex. Modification with **D-isoT** at position 12 broke the critical interactions for the binding with thrombin Arg-75 and Arg-77A.

Based on the results of single **D-/L-isoT** modified **TBA**, the combined bis-**D-/L-isoT** modification produced **TBA-3L7D** and **TBA-7D12L**, which showed compared or increased thrombin bonding, but only the later show compared clotting inhibitory activity with **TBA-12L**.

4. Conclusions

We used **D-/L-isoT** to modify the G-quadruplex aptamer and studied the thermodynamic stability, thrombin binding, and blood clotting inhibiting activity of the modified **TBAs**. **L-isoT** introduced at positions T3, T9 or T12 and **D-isoT** at position T7 stabilized the G-quadruplex structure, increased the binding with thrombin, and exhibited higher clotting inhibitory activity than the parent **TBA**. Moreover, **D-/L-isoT** modifications at those positions maintained the overall aptamer structure and the antiparallel G-quadruplex topology. Specifically, modified aptamer **TBA-3L**, **TBA-7D**, **TBA-9L**, **TBA-12L**, **TBA-3L7D**, and **TBA-7D12L** showed increased blood clotting inhibitory activities. Modification at T12 with **L-isoT** showed the most dramatic effect, suggesting T12 is important in the interaction with thrombin, and conformation alteration in this position could improve the biological effect of **TBA**. Moreover, **TBA-7D12L** showed similar biological effect as **TBA-12L**, which mean that the second combination of thrombin to **TBA** was relative weak interaction and would not result in additional biological effects. Our results support that modification with **D-/L-isoT** is a promising strategy to enhance the stability and biological activity of **TBA**.

View Article Online
Organic & Biomolecular Chemistry
EDGE Atricle

There is close relationship between the structure of **TBA** variants and bioactivity, but that doesn't mean the formation of a stable G4 structure will certainly have better activity. Forming a stable G4 structure is only the basic condition for **TBA** to play bioactivity. The NMR model of **TBA/**thrombin bonding could be more close to the actual conformation. Our study also suggested that **TBA** might interact with two thrombin molecules through the TT loops (T3T4, T12T13) and TGT loop, but the second bonding didn't show additional biological effect.

Acknowledgement

This work was supported by the Ministry of Science and Technology of China (Grant No. 2012CB720604, 2012AA022501), the National Natural Science Foundation of China (Grant No. 21332010, 20932001).

References

1. J. E. Johnson, J. S. Smith, M. L. Kozak and F. B. Johnson, *Biochimie,* 2008, **90**, 1250-1263.
2. S. Burge, G. N. Parkinson, P. Hazel, A. K. Todd and S. Neidle, *Nucleic Acids Res.,* 2006, **34**, 5402-5415.
3. A. Siddiqui-Jain, C. L. Grand, D. J. Bearss and L. H. Hurley, *Proc. Natl. Acad. Sci. USA*, 2002, **99**, 11593-11598.
4. J. L. Huppert and S. Balasubramanian, *Nucleic Acids Res.,* 2005**, 33***,* 2908-2916.
5. Y. Xu, K. Kaminaga and M. Komiyama, *J. Am. Chem. Soc.,* 2008, **130**, 11179-11184.
6. J. L. Huppert, *Chem. Soc. Rev.,* 2009, **37**, 1375-1384.
7. Z. S. Wu, P. Hu, H. Zhou, G. Shen and R.Yu, *Biomaterials,* 2010, **31**, 1918-1924.
8. H. X. Jiang, D. M. Kong and H. X. Shen, *Biosens. Bioelectron,* 2014, **55**, 133-138.
9. Z. Chen, Y. Tan, C. Zhang, L. Yin, H. Ma, N. Ye, H. Qiang and Y. Lin, *Biosens. Bioelectron,* 2014, **56**, 46-50.
10. K. H. Leung, H. Z. He, H. J. Zhong, L. Lu, D. S. H. Chan, D. L. Ma and C. H. Leung, *Methods,* 2013, **64**, 224-228.
11. Y. He, X. Wang, Y. Zhang, F. Gao, Y. Li, H. Chen and L. Wang, *Talanta,* 2013, **116**, 816-821.
12. J. Wu, C. Wang, X. Li, Y. Song, W. Wang, C. Li, J. Hu, Z. Zhu, J. Li and W. Zhang, *PloS One,* 2012, **7**, e46393.
13. T. Li, E. Wang and S. Dong, *Chem. Commun.,* 2008, **31**, 3654-3656.
14. L. C. Bock, L. C. Griffin, J. A. Latham, E. H. Vermaas and J. J.Toole, *Nature,* 1992, **355**, 564-566.
15. J. A. Kelly, J. Feigon and T. O. Yeates, *J. Mol. Biol.,* 1996, **256**, 417-422.
16. R. F. Macaya, P. Schultze, F. W. Smith, J. A. Roe and J. Feigon, *Proc. Natl. Acad. Sci. USA,* 1993, **90**, 3745-3749.

View Article Online
Organic & Biomolecular Chemistry
EDGE Atricle

17. K. Y. Wang, S. H. Krawczyk, N. Bischofberger, S. Swaminathan and P. H. Bolton, *Biochemistry,* 1993, **32**, 11285-11292.
18. K. Padmanabhan, K. P. Padmanabhan, J. D. Ferrara, J. E. Sadler and A. Tulinsky, *J. Biol. Chem.,* 1993, **268**, 17651-17654.
19. P. Schultze, R. F. Macaya and J. Feigon, *J. Mol. Biol.,* 1994, **235**, 1532-1547.
20. K. Padmanabhan and A. Tulinsky, *Acta Crystallogr. D Biol. Crystallogr.,* 1996, **52**, 272-282.
21. I. R. Krauss, A. Merlino, A. Randazzo, E. Novellino, L. Mazzarella and F. Sica, *Nucleic Acids Res.,* 2012, **40**, 8119-8128.
22. I. Russo Krauss, A. Merlino, C. Giancola, A. Randazzo, L. Mazzarella and F. Sica, *Nucleic Acids Res.,* 2011, **39**, 7858-7867.
23. A. Pasternak, F. J. Hernandez, L. M. Rasmussen, B. Vester and J. Wengel, *Nucleic Acids Res.,* 2011, **39**, 1155-1164.
24. S. M. Raviv, A. Horvath, J. Aradi, Z. Bagoly, F. Fazakas, Z. Batta, L. Muszbek, and J. Harsfalvi, *J. Thromb. Homeost.,* 2008, **6**, 1764-1771.
25. A. Virno, A. Randazzo, C. Giancola, M. Bucci, G. Cirino and L. Mayol, *Bioorg. Med. Chem.,* 2007, **15**, 5710-5718.
26. a. M. Scuotto, M. Persico, M. Bucci, V. Vellecco, N. Borbone, E. Morelli, G. Oliviero, E. Novellino, G. Piccialli, G. Cirino, M. Varra, C. Fattorusso and L. Mayol, *Org. Biomol. Chem.*, 2014, **12**, 5235-5242. b. N. Borbone, M. Bucci, G. Oliviero, E. Morelli, J. Amato, V. D'Atri, S. D'Errico, V. Vellecco, G. Cirino, G. Piccialli, C. Fattorusso, M. Varra, L. Mayol, M. Persico, M. Scuotto, *J. Med. Chem.*, 2012, **55**, 10716-10728. c. T. Coppola, M. Varra, G. Oliviero, A. Galeone, G. D'Isa, L. Mayol, E. Morelli, M.-R. Bucci, V. Vellecco, G. Cirino, N. Borbone, *Bioorg. Med. Chem.*, 2008, **16**, 8244-8253.
27. S. R. Nallagatla, B. Heuberger, A. Haque and C. Switzer, *J. Comb. Chem.,* 2009, **11**, 364-369.
28. a. B. Sacca, L. Lacroix and J. L.Mergny, *Nucleic Acids Res.,* 2005, **33**, 1182-1192. b. C.-F. Tang and R. H. Shafer, *J. Am. Chem. Soc.,* 2006, **128**, 5966-5973.
29. M. Zaitseva, D. Kaluzhny, A. Shchyolkina, O. Borisova, I. Smirnov and G. Pozmogova, *Biophys. Chem.,* 2010, **146**, 1-6.
30. L. Martino, A. Virno, A. Randazzo, A. Virgilio, V. Esposito, C. Giancola, M. Bucci, G. Cirino and L. Mayol, *Nucleic Acids Res.,* 2006, **34**, 6653-6662.
31. B. Pagano, L. Martino, A. Randazzo and C. Giancola, *Biophys. J.,* 2008, **94**, 562-569.
32. I. Smirnov and R. H. Shafer, *Biochemistry,* 2000, **39**, 1462-1468.
33. a. H. W. Yu, L. R. Zhang, J. C. Zhou, L. T. Ma and L. H. Zhang, *Bioorg. Med. Chem.,* 1996, **4**, 609-614. b. H. Y. Zhang, X. J. Wu, H. W. Yu, L. T. Ma and L. H. Zhang, *Chin. Chem. Letts.,* 1996, **12**, 1089-1090. c. Z. J. Yang, H. W. Yu, J. M. Min, L. T. Ma and L. H. Zhang, *Tetrahedron: Asymmetry*, 1997, **8**, 2739-2747.
34. a. Z. J. Yang, H. Y. Zhang, J. M. Min, L. T. Ma and L. H. Zhang, *Helv. Chim. Acta,* 1999, **82**, 2037-2043. b. Z. Guan, X. B. Tian, L. R. Zhang, J. M. Min and L. H. Zhang, *Helv. Chim. Acta,* 2002, **85**, 1479-1484. c. F. Wang, Y. Chen, Y. Huang, H. W. Jin, L. R. Zhang, Z. J. Yang and L. H. Zhang, *Sci. China Chem.,* 2012, **55**, 1-10. d. Z. L. Wang, J. F. Shi, H. W. Jin, L. R. Zhang, J. F. Lu and L. H. Zhang, *Bioconjugate Chem.,* 2005, **16**, 1081-1087. e. J. Zhang, Y. Chen, Y. Huang, H. W. Jin, R. P. Qiao, L. Xing, L. R. Zhang, Z. J. Yang and L. H. Zhang, *Org. Biomol. Chem.,* 2012, **10**, 7566-7577. f. Z. S. Li, R. P. Qiao, Q. Du, Z. J. Yang, L. R. Zhang, P. Z. Zhang, Z. C. Liang and L. H. Zhang, *Bioconjugate Chem.,* 2007, **18**, 1017-24. g. Y. Huang, Z. Chen, Y. Chen,

H. Zhang, Y.C. Zhang, Y.L. Zhao, Z.J. Yang and L.H. Zhang, *Bioconjugate Chem.,* 2013, **24**, 951-959. h. J. Chen, L.R. Zhang, J. M. Min and L.H. Zhang, *Nucleic Acids Res.,* 2002, **30**, 3005-3014.

35. L. D. Sun, H. W. Jin, X. Y. Zhao, Z. M. Liu, Y. F. Guan, Z. J. Yang, L. R. Zhang and L. H. Zhang, *ChemMedChem*, 2014, **9**, 993-1001.
36. AMBER 11 (2010), University of California, San Francisco.
37. Gaussian 09 (2009), Gaussian, Inc., Wallingford CT.
38. T. Darden, D. York, and L. Pedersen, *J. Chem. Phys.,* 1993, **98**, 10089-10092.
39. Discovery Studio 2.5 (2009), Accelrys Inc., San Diego.
40. P. A. Kollman, I. Massova, C. Reyes, B. Kuhn, S. H. Huo, L. Chong, M. Lee, T. Lee, Y. Duan, W. Wang, O. Donini, P. Cieplak, J. Srinivasan and D. A. Case, *Acc. Chem. Res.,* 2000, **33**, 889-897.
41. J. M. Wang, T. J. Hou, X. J. Xu, *Curr. Comput-Aid Drug,* 2006, **2**, 287-306.
42. G. Zagotto, C. Sissi, S. Moro, D. Dal Ben, G. N. Parkinson, K. R. Fox, S. Neidle and M. Palumbo, *Bioorg. Med. Chem.,* 2008, **16**, 354-361.
43. L. Bonifacio, F. C. Church and M. B.Jarstfer, *Int. J. Mol. Sci.,* 2008, **9**, 422-433.